
Sparse Parallel Training of Hierarchical Dirichlet Process Topic Models

Alexander Terenin*
Imperial College London (UK)
A.TERENIN17@IMPERIAL.AC.UK

Måns Magnusson
Aalto University (FI)
MANS.MAGNUSSON@AALTO.FI

Leif Jonsson
Ericsson (SE)
LEIF.JONSSON@ERICSSON.COM

Abstract

Nonparametric extensions of topic models such as Latent Dirichlet Allocation, including Hierarchical Dirichlet Process (HDP), are often studied in natural language processing. Training these models generally requires use of serial algorithms, which limits scalability to large data sets and complicates acceleration via use of parallel and distributed systems. Most current approaches to scalable training of such models either don't converge to the correct target, or are not data-parallel. Moreover, these approaches generally do not utilize all available sources of sparsity found in natural language – an important way to make computation efficient. Based upon a representation of certain conditional distributions within an HDP, we propose a doubly sparse data-parallel sampler for the HDP topic model that addresses these issues. We benchmark our method on a well-known corpora (PubMed) with 8m documents and 768m tokens, using a single multi-core machine in under three days.

1 Introduction

Topic models are a widely-used class of models in natural language processing that allow practitioners to identify latent semantic themes occurring in large bodies of text. Hierarchical Bayesian discrete mixture models such as Latent Dirichlet Allocation (LDA) [4] and its many nonparametric extensions [5, 12, 20, 23, 24] are ubiquitous within the field. These models usually combine categorical likelihoods with conjugate Dirichlet or Dirichlet process priors, and are trained via various forms of Bayesian learning. To train these models in massively parallel settings, the training algorithm needs to satisfy two requirements.

1. Expose sufficient parallelism that the hardware can take advantage of.
2. Utilize sparsity found in natural language [31] to control memory requirements and computational complexity.

In this work, we focus on the *Hierarchical Dirichlet process* (HDP) topic model of Teh et al. [24], which we review in Section 2. This model is perhaps the simplest non-trivial extension of LDA to the nonparametric setting – its parallel implementation provides a blueprint for designing massively parallel training algorithms in more complicated settings such as topic models with Pitman-Yor priors [23], nonparametric dynamic topic models [1], tree-based extensions [5, 12], and others.

*Website: [HTTPS://AVT.IM/](https://avt.im/)

Symbol	Description	Symbol	Description
V	Vocabulary size	$\Psi : 1 \times \infty$	Global distribution over topics
D	Total number of documents	$\Theta : D \times \infty$	Document-topic probabilities
N	Total number of tokens	$\theta_d : 1 \times \infty$	Topic probabilities for document d
$v(i)$	Word type for token i	$\mathbf{m} : D \times \infty$	Document-topic sufficient statistic
$d(i)$	Document for token i	$\Phi : \infty \times V$	Topic-word probabilities
$w_{i,d}$	Token i in document d	$\phi_k : 1 \times V$	Word probabilities for topic k
$b_{i,d}$	Global topic draw indicator for $w_{i,d}$	$\mathbf{n} : \infty \times V$	Topic-word sufficient statistic
$z_{i,d}$	Topic indicator for token i in d	$\mathbf{l} : 1 \times \infty$	Global topic latent sufficient statistic
K^*	Index for implicitly-represented topics	α, β, γ	Prior concentration for θ_d, ϕ_k, Ψ

Table 1: Notation for the HDP topic model. Sufficient statistics are conditional on algorithm’s current iteration. Bold symbols refer to matrices, bold italics refer to vectors, possibly countably infinite.

Parallel approaches to training HDPs have been previously introduced by a number of authors, including Newman et al. [19], Wang et al. [28], Williamson et al. [29], and Chang and Fisher [8]. Gal and Ghahramani [10] have pointed out some of these methods can suffer from load-balancing issues which limit their available parallelism and scalability. The largest-scale benchmark of parallel HDP training performed thus far to our awareness is by Chang and Fisher [8] on the 100m-token *NYTimes* corpora.

Our contributions are as follows. We propose an augmented representation of the HDP under which the topic indicators can be sampled in parallel over documents. We prove that the global topic distribution Ψ , which is assigned a Griffiths-Engen-McCloskey (GEM) [22] prior under this representation, is conditionally conjugate given an auxiliary parameter \mathbf{l} . We develop fast sampling schemes for Ψ and \mathbf{l} , thereby directly extending the parallel partially collapsed Gibbs sampler of Magnusson et al. [16] and Terenin et al. [25] from LDA to HDP. The proposed algorithm is doubly sparse: it has per-iteration complexity which depends on the minima of two sparsity terms, and thus takes advantage of both document-topic and topic-word sparsity simultaneously.

2 Partially collapsed Gibbs sampling for hierarchical Dirichlet processes

The Hierarchical Dirichlet Process topic model [24] begins with a global distribution Ψ over topics. Documents are assumed exchangeable – for each document d , the associated topic distribution θ_d follows a Dirichlet process centered at Ψ . Each topic is associated with a distribution of tokens ϕ_k . Within each document, tokens are assumed exchangeable (bag of words) and assigned to topic indicators $z_{i,d}$. For a given data set, we observe the tokens $w_{i,d}$.

Summarizing everything, we arrive at the GEM representation of a hierarchical Dirichlet process, given by equation (19) of Teh et al. [24] as

$$\Psi \sim \text{GEM}(\gamma) \tag{1}$$

$$\theta_d \mid \Psi \sim \text{DP}(\alpha, \Psi) \qquad \phi_k \sim \text{Dir}(\beta) \tag{2}$$

$$z_{i,d} \mid \theta_d \stackrel{\text{iid}}{\sim} \text{Discrete}(\theta_d) \qquad w_{i,d} \mid z_{i,d}, \Phi \sim \text{Discrete}(\phi_{z_{i,d}}) \tag{3}$$

where α, β, γ are prior hyperparameters.

2.1 Intuition and augmented representation

At a high level, our strategy for constructing a scalable sampler is as follows. Conditional on Ψ , the likelihood in equation (1) is the same as that of LDA. Using this observation, the Gibbs step for \mathbf{z} , which is the largest component of the model, can be handled efficiently by leveraging insights on sparse parallel sampling from the well-studied LDA literature [15, 16, 25, 30]. For this strategy to succeed, we need to ensure that all Gibbs steps involved in the HDP under this representation are analytically tractable and can be computed efficiently. For this, the representation needs to be slightly modified.

To begin, we integrate each θ_d out of the model, which by conjugacy [3] yields a Pólya sequence for each \mathbf{z}_d . By definition, given in Appendix A, this sequence is a mixture distribution with respect to a

set of Bernoulli random variables \mathbf{b}_d , each representing whether $w_{i,d}$ was drawn from Ψ or from a repeated draw in the Pólya urn. Thus, the HDP model admits the representation

$$\Psi \sim \text{GEM}(\gamma) \quad (4)$$

$$b_{i,d} \sim \text{Ber}\left(\frac{\alpha}{i-1+\alpha}\right) \quad \phi_k \sim \text{Dir}(\beta) \quad (5)$$

$$z_d \mid \mathbf{b}_d, \Psi \sim \text{PS}(\Psi, \mathbf{b}_d) \quad w_{i,d} \mid z_{i,d} \sim \text{Discrete}(\phi_{z_{i,d}}) \quad (6)$$

where $\text{PS}(\Psi, \mathbf{b}_d)$ is defined in Appendix A. This representation defines a posterior distribution over $\mathbf{z}, \Phi, \Psi, \mathbf{b}$ for the HDP. To derive a Gibbs sampler, we proceed to calculate its full conditionals.

2.2 Full conditionals for \mathbf{z}, Φ , and \mathbf{b}

The full conditionals $\mathbf{z} \mid \Phi, \Psi$ and $\Phi \mid \mathbf{z}, \Psi$, with \mathbf{b} marginalized out, are essentially identical to those in partially collapsed LDA [16, 25]. They are

$$\mathbb{P}(z_{i,d} = k \mid \mathbf{z}_{-i,d}, \Phi, \Psi) \propto \phi_{k,v(i)} \left[\alpha \Psi_k + m_{d,k}^{-i} \right] \quad \phi_k \mid \mathbf{z} \sim \text{Dir}(\beta + \mathbf{n}_k) \quad (7)$$

where $m_{d,k}^{-i}$ denotes the document-topic sufficient statistic with index i removed. Note that the number of possible topics and full conditionals $\phi_k \mid \mathbf{z}$ here is countably infinite. The full conditional for each $b_{i,d}$ is

$$\mathbb{P}(b_{i,d} = 1 \mid \mathbf{z}_d, \Psi, \mathbf{b}_{-i,d}) = \frac{\alpha \Psi_{z_{i,d}}}{\alpha \Psi_{z_{i,d}} + \sum_{j=1}^i \mathbb{1}_{z_{j,d}}(z_{i,d})}. \quad (8)$$

The derivation, based on a direct application of Bayes' Rule with respect to the probability mass function of the Pólya sequence, is given in Appendix A.

2.3 The full conditional for Ψ

To derive the full conditional for Ψ , we examine the prior and likelihood components of the model. It is shown in Appendix A that the likelihood term $\mathbf{z}_d \mid \mathbf{b}_d, \Psi$ may be written

$$p(\mathbf{z}_d \mid \mathbf{b}_d, \Psi) = \underbrace{\prod_{\substack{i=1 \\ b_{i,d} \neq 1}}^{N_d} \sum_{j=1}^{i-1} \frac{1}{i-1} \mathbb{1}_{z_{j,d}}(z_{i,d})}_{\text{doesn't enter posterior}} \prod_{\substack{i=1 \\ b_{i,d}=1}}^{N_d} \prod_{k=1}^{\infty} \Psi_k^{\mathbb{1}_k(z_{i,d})}. \quad (9)$$

The first term is a multiplicative constant independent of Ψ and vanishes via normalization. Thus, the full conditional $\Psi \mid \mathbf{z}, \mathbf{b}$ depends on \mathbf{z} and \mathbf{b} only through the sufficient statistic \mathbf{l} defined by

$$l_k = \sum_{d=1}^D \sum_{\substack{i=1 \\ b_{i,d}=1}}^{N_d} \mathbb{1}_{z_{i,d}=k} \quad (10)$$

and so we may suppose without loss of generality that the likelihood term is categorical. Under these conditions, we prove, via a measure-theoretic argument, that the full conditional for Ψ admits a stick-breaking representation.

Proposition 1. *Without loss of generality, suppose we have*

$$\Psi \sim \text{GEM}(\gamma) \quad \mathbf{x} \mid \Psi \sim \text{Discrete}(\Psi). \quad (11)$$

Then $\Psi \mid \mathbf{x}$ is given by

$$\Psi_k = \varsigma_k \prod_{i=1}^{k-1} (1 - \varsigma_i) \quad \varsigma_k \sim \text{B}(a_k^{(\Psi)}, b_k^{(\Psi)}) \quad a_k^{(\Psi)} = 1 + l_k \quad b_k^{(\Psi)} = \gamma + \sum_{i=k+1}^{\infty} l_i \quad (12)$$

where \mathbf{l} is the empirical distribution of \mathbf{x} .

Proof. Appendix B. ■

Putting these ideas together, we define an infinite-dimensional parallel Gibbs sampler for the HDP.

Algorithm 1 (Infinite-dimensional partially collapsed Gibbs sampling for the HDP topic model).
Repeat until convergence.

- Sample $\phi_k \sim \text{Dir}(\mathbf{n}_k + \beta)$ in parallel over topics for $k = 1, \dots, \infty$.
- Sample $z_{i,d} \propto \phi_{k,v(i)} \alpha \Psi_k + \phi_{k,v(i)} m_{d,k}^{-i}$ in parallel over documents for $d = 1, \dots, D$.
- Sample $b_{i,d}$ according to Equation (8) in parallel over documents for $d = 1, \dots, D$.
- Sample Ψ according to Proposition 1.

Algorithm 1 is completely parallelizable, but cannot be implemented as stated due to the infinite number of full conditionals for Φ , as well as the infinite product used in sampling Ψ . We proceed to bypass these issues by introducing an approximate finite-dimensional sampling scheme.

2.4 Finite-dimensional sampling of Ψ and Φ

By way of assuming $\Psi \sim \text{GEM}(\gamma)$, an HDP assumes that an infinite number of topics are present in the model a priori, with the number of tokens per topic decreases rapidly with the topic’s index in a manner controlled by γ . Thus, we expect under the model that a topic with a sufficiently large index K will contain no tokens with high probability.

We thus propose to approximate Ψ in a finite-dimensional manner by projecting its tail onto a single flag topic K^* , which stands for all topics not explicitly represented as part of the computation. Following Ishwaran and James [13], this can be done by deterministically setting $\zeta_{K^*} = 1$ in Proposition 1, which, as part of its proof, implies the approximation is convergent and well-posed.

Once this is done, Ψ becomes a finite vector of length K^* , and only K^* rows of Φ need to be explicitly instantiated as part of the computation. This allows the algorithm to be defined on a fixed finite state space, simplifying bookkeeping and implementation.

From a computational efficiency perspective, the resulting value K^* takes the place of K in partially collapsed LDA – however, it *cannot* be interpreted as the number of topics in the sense of LDA. Indeed, LDA implicitly assumes that $\Psi = \text{U}(1, \dots, K)$ deterministically – i.e. that every topic is assumed a priori to contain the same number of tokens, whereas the HDP model assumes otherwise by letting $\Psi \sim \text{GEM}(\gamma)$.

If we allow the state space to be resized when topic K^* is sampled, then following Papaspiliopoulos and Roberts [21] it is possible to develop truncation schemes which introduce no error. Since this results in more complicated bookkeeping, we instead fix K^* and defer such considerations to future work. We recommend setting K^* to be sufficiently large that it does not significantly affect the model’s behavior, which can be checked by tracking the number of tokens assigned to topic K^* .

2.5 Sparse sampling of Φ and z

To be efficient, a topic model needs to utilize the sparsity found in natural language as much as possible. In our case, the two main sources of sparsity are as follows.

1. *Document-topic sparsity*: most documents will only contain a handful of topics.
2. *Topic-word sparsity*: most word types will not be present in most topics.

From this, we expect the document-topic sufficient statistic \mathbf{m} and topic-word sufficient statistic \mathbf{n} to contain many zeros. We seek to use this to reduce sampling complexity. Our starting point is the Poisson Pólya Urn-based sampler of Terenin et al. [25], which presents a Gibbs sampler for LDA with computational complexity that depends on the minima of two sparsity coefficients representing document-topic and topic-word sparsity – such algorithms are termed *doubly sparse*. The key idea is to approximate the Dirichlet full conditional for ϕ_k with a Poisson Pólya Urn distribution defined by

$$\phi_{k,v} = \frac{\varphi_{k,v}}{\sum_{v=1}^V \varphi_{k,v}} \quad \varphi_{k,v} \sim \text{Pois}(\beta_{k,v} + n_{k,v}) \quad (13)$$

for $v = 1, \dots, V$. This distribution is discrete, so Φ becomes a sparse matrix. The approximation is accurate even for small values of $n_{k,v}$, and approximation error is proven by Terenin et al. [25] to vanish for large data sets in the sense of weak convergence.

In the case where β is uniform, we can further use sparsity to accelerate sampling $\varphi_{k,v}$. Since a sum of Poisson random variables is Poisson, we can split $\varphi_{k,v} = \varphi_{k,v}^{(\beta)} + \varphi_{k,v}^{(\mathbf{n})}$. We then sample $\varphi_{k,v}^{(\beta)}$ sparsely by introducing a Poisson process and sampling its points uniformly, and sample $\varphi_{k,v}^{(\mathbf{n})}$ sparsely by iterating over nonzero entries of \mathbf{n} .

For z , the full conditional

$$\mathbb{P}(z_{i,d} = k \mid \mathbf{z}_{-i,d}, \Phi, \Psi) \propto \phi_{k,v(i)} \left[\alpha \Psi_k + m_{d,k}^{-i} \right] \quad (14)$$

$$\propto \underbrace{\phi_{k,v(i)} \alpha \Psi_k}_{(a)} + \underbrace{\phi_{k,v(i)} m_{d,k}^{-i}}_{(b)} \quad (15)$$

is essentially identical to the one in Pólya Urn LDA – the only difference is the presence of Ψ_k . As Ψ_k only enters the expression through component (a) and is identical for all $z_{i,d}$, it can be absorbed at each iteration directly into the Walker alias tables [15, 26] – see Magnusson et al. [16] for details. Component (b) can be computed efficiently by utilizing sparsity of Φ and \mathbf{m} and iterating over whichever has fewer non-zero entries – see Terenin et al. [25] for details.

2.6 Direct sampling of l

Rather than sampling \mathbf{b} , whose size will grow linearly with the number of documents, we introduce a scheme for sampling the sufficient statistic l directly. Observe that

$$l_k = \sum_{d=1}^D \sum_{\substack{i=1 \\ b_{i,d}=1}}^{N_d} \mathbb{1}_{z_{i,d}=k} = \sum_{d=1}^D \sum_{\substack{i=1 \\ z_{i,d}=k}}^{N_d} \mathbb{1}_{b_{i,d}=1}. \quad (16)$$

By definition of $b_{i,d}$, we have

$$\sum_{\substack{i=1 \\ z_{i,d}=k}}^{N_d} \mathbb{1}_{b_{i,d}=1} = \sum_{j=1}^{m_{d,k}} b_{j,d,k} \quad b_{j,d,k} \sim \text{Ber} \left(\frac{\Psi_k \alpha}{\Psi_k \alpha + j - 1} \right). \quad (17)$$

Summing this expression over documents, we obtain

$$l_k = \sum_{j=1}^{\max_d m_{d,k}} c_{j,k} \quad c_{j,k} \sim \text{Bin} \left(D_{k,j}, \frac{\Psi_k \alpha}{\Psi_k \alpha + j - 1} \right) \quad (18)$$

where $D_{k,j}$ is the total number of documents with $m_{d,k} \geq j$. Since $m_{d,k} = 0$ for all topics k without any tokens assigned, we only need to sample l for topics that have tokens assigned to them. The complexity of sampling l via this expression is constant with respect to the number of documents, and depends instead on the maximum number of tokens per document.

To handle the bookkeeping necessary for computing $D_{k,j}$, we introduce a sparse matrix \mathbf{d} of size $K \times \max_d N_d$ whose entries $d_{k,p}$ are the number of documents for topic k that have a total of p topic indicators assigned to them. We increment \mathbf{d} once \mathbf{z}_d been sampled by iterating over non-zero elements in \mathbf{m}_d . We then compute $D_{k,j}$ as the *reverse cumulative sum* of the rows of \mathbf{d} .

Putting all of these ideas together, we obtain the following algorithm.

Algorithm 2 (Poisson Pólya urn partially collapsed Gibbs sampling for the HDP topic model). *Repeat until convergence.*

- Sample $\phi_k \sim \text{PPU}(\mathbf{n}_k + \beta)$ in parallel over topics for $k = 1, \dots, K^*$.
- Sample $z_{i,d} \propto \phi_{k,v(i)} \alpha \Psi_k + \phi_{k,v(i)} m_{d,k}^{-i}$ in parallel over documents for $d = 1, \dots, D$.
- Sample l_k according to Equation (18) in parallel over topics for $k = 1, \dots, K^*$.
- Sample Ψ according to Proposition 1, except with $\varsigma_{K^*} = 1$.

Algorithm 2 is sparse, massively parallel, and contains no infinite computations in any of its steps. The Gibbs steps for Φ converge in distribution [25] to the true Gibbs steps as $N \rightarrow \infty$, and the Gibbs step for Ψ converges almost surely [13] to the true Gibbs step as $K^* \rightarrow \infty$.

2.7 Computational complexity

We now examine the per-iteration computational complexity of Algorithm 2. To proceed, we fix K^* and maximum document size $\max_d N_d$, and relate the vocabulary size V with the number N of total words as follows.

Assumption (Heaps’ Law). *The number of unique words in a corpus follows Heaps’ law [11] $V = \xi N^\zeta$ with constants $\xi > 0$ and $\zeta < 1$.*

The per-iteration complexity of Algorithm 2 is equal to the sum of the per-iteration complexity of sampling its components. The sampling complexities of Ψ and l are constant with respect to the number of tokens, and the sampling complexity of Φ has been shown by Magnusson et al. [16] to be negligible under the given assumptions. Thus, it suffices to consider z .

At a given iteration, let $K_{d(i)}^{(m)}$ be the number of existing topics in document d associated with word token i , and let $K_{v(i)}^{(\Phi)}$ be the number of nonzero topics in the row of Φ corresponding to word token i . It follows immediately from the argument given by Terenin et al. [25] that the per-iteration complexity of sampling a single topic indicator z_i is

$$\mathcal{O}\left[\min\left\{K_{d(i)}^{(m)}, K_{v(i)}^{(\Phi)}\right\}\right]. \quad (19)$$

Algorithm 2 is thus a doubly sparse algorithm.

3 Performance results

To study the performance of the *partially collapsed* sampler – Algorithm 2 – we implemented it in Java using the open-source *Mallet*² [17] topic modeling framework. We ran it on the *CGCBIB*, *NeurIPS*, and *PubMed* corpora³, which are summarized in Table 2. Prior hyperparameters were set to $\alpha = 0.1, \beta = 0.01, \gamma = 1$. We set $K^* = 1000$ and observed no tokens ever allocated to topic K^* . Data was preprocessed with default Mallet stop-word removal, minimum document size of 10, and a rare word limit of 10. Following standard practice for the HDP topic model [8, 24, 28, 29], the algorithm was initialized with one topic. Total runtime for each experiment is given in Table 2.

To assess Algorithm 2 in a small-scale setting and compare it to the widely-studied fully collapsed *direct assignment* sampler of Teh et al. [24], which is not parallel, we ran 100 000 iterations of both methods on CGCBIB. We selected this corpora because it was among the larger corpora for which it was feasible to run our direct assignment reference implementation within one week. Computation was performed on an Apple MacBook Pro laptop, which has a 6-core i7-8850H CPU with 16GB RAM.

Trace plots for the log marginal likelihood for z given Ψ and number of active topics, i.e. those topics assigned at least one token, can be seen in Figure 1(a) and Figure 1(b), respectively. The direct assignment algorithm converges slower, but achieves a slightly better local optima in terms of marginal log-likelihood, compared to our method. This indicates that it may stabilize at a different local optima, and may represent a potential limitation of the partially collapsed sampler in settings where non-parallel methods are practical.

To better understand distributional differences between the algorithms, we examined the number of tokens per topic, which can be seen in Figure 1(c). The partially collapsed sampler is seen to assign

²See [HTTP://MALLET.CS.UMASS.EDU](http://mallet.cs.umass.edu) and [HTTPS://GITHUB.COM/LEJON/PARTIALLYCOLLAPSEDLDA](https://github.com/lejon/partiallycollapsedlda).

³CGCBIB can be found at [HTTPS://GITHUB.COM/LEJON/PARTIALLYCOLLAPSEDLDA](https://github.com/lejon/partiallycollapsedlda).

NeurIPS and PubMed can be found at [HTTPS://ARCHIVE.ICS.UCI.EDU/ML/DATASETS/BAG+OF+WORDS](https://archive.ics.uci.edu/ml/datasets/bag+of+words).

Corpus	V	D	N	Iterations	Threads	Runtime
CGCBIB	6 079	5 940	570 370	100 000	12	2.7 hours
NeurIPS	12 419	1 499	1 894 051	255 500	8	24 hours
PubMed	89 987	8 199 999	768 434 972	20 000	20	65.2 hours

Table 2: Corpora used in experiments, together with compute configuration.

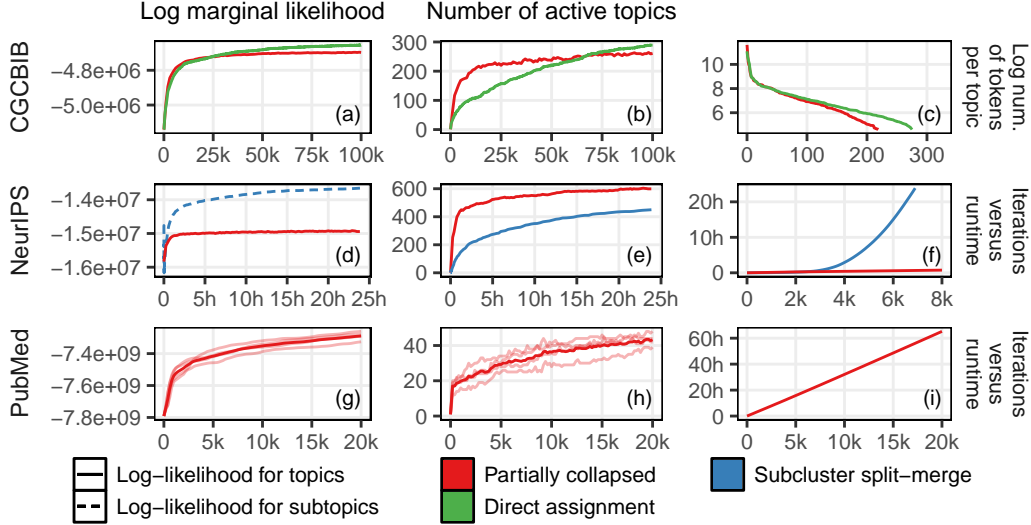


Figure 1: Trace plots for log-likelihood, number of active topics, and additional metrics for CGCBIB, NeurIPS, and PubMed. Per-iteration scale is used for CGCBIB and PubMed, realtime scale is used for NeurIPS. Algorithms used are partially collapsed HDP for all corpora, direct assignment HDP for CGCBIB, and subcluster split-merge HDP for NeurIPS. Where multiple runs are present, individual traces are partially transparent, and their mean is opaque.

more tokens to smaller topics, indicating that it stabilizes at a local optima with slightly broader semantic themes.

To visualize the effect this has on the topics, we examined the most common words for each topic. Since the algorithms generate too many topics to make full examination practical, we instead compute a quantile summary with five topics per quantile. This is computed by ranking all topics by number of tokens, choosing the five closest topics to the 100%, 75%, 50%, 25%, 5% quantiles in the ranking, and computing their top words. This gives a representative view of the algorithm’s output for large, medium, and small topics. Results may be seen in Appendix C – we find the direct assignment and partially collapsed samplers to be largely comparable, with substantial overlap in top words for common topics.

To assess Algorithm 2 in a more demanding setting and compare against previous parallel state-of-the-art, we ran it and the parallel *subcluster split-merge* algorithm of Chang and Fisher [8] on the NeurIPS corpora. The subcluster split-merge algorithm is designed to converge with fewer iterations, but is more costly to run per iteration, so for both algorithms we used a fixed computational budget of 24 hours of wall-clock time. Computation was performed on a system with a 4-core i7-4790 CPU and 8GB RAM.

Results can be seen in Figure 1(d) – note that the subcluster split-merge algorithm is parametrized using *sub-topic indicators* and *sub-topic probabilities*, so its numerical log-likelihood values are not directly comparable to ours and should be *interpreted purely to assess convergence*. Algorithm 2 stabilizes much faster with respect to both the number of active topics in Figure 1(d), and marginal log-likelihood in Figure 1(e). The subcluster split-merge algorithm is only able to add new topics one-at-a-time, whereas our algorithm can create multiple new topics per iteration – we hypothesize this difference leads to faster convergence for Algorithm 2.

In Figure 1(f), we observe that the amount of compute time per iteration increases substantially for the subcluster split-merge method as it discovers more topics. For Algorithm 2, this stays approximately constant for its entire runtime.

To evaluate the topics produced by the algorithms, we again examined the most common words for each topic via a quantile summary, which may be seen in Appendix D. We find that the subcluster split-merge algorithm appears to generate topics with slightly more semantic overlap compared to Algorithm 2, but has otherwise produced comparable output.

Finally, to assess scalability, we ran 20 000 iterations of Algorithm 2 on PubMed, which contains 768m tokens. To our knowledge, this dataset is an order of magnitude larger than any datasets used in previous MCMC-based approaches for the HDP. Computation was performed on a standard compute node at the Triton scientific compute cluster at Aalto University, which has 2x10-core Xeon E5 2680v2 CPUs with hyper-threading disabled and 64GB of RAM. The experiment was repeated four times to assess variability. Marginal log-likelihood and the number of active topics can be seen in Figure 1(g) and Figure 1(h).

To evaluate the topics discovered by the algorithm, we examined their most common words – these may be seen for every topic in Appendix E. We find by inspection that essentially all topics generated by the algorithm look reasonable and compelling. In particular, there appear to be virtually no duplicate topics, and few topics that contain multiple clearly-unrelated semantic concepts which should be split up. This suggests that the algorithm captures the underlying semantics well. We suspect the topic estimates for PubMed are particularly sharp compared to other corpora due to the large number of tokens present.

4 Discussion

In this work, we introduce the parallel partially collapsed Gibbs sampler – Algorithm 1 – for the HDP topic model, which converges to the correct target distribution. We propose a doubly sparse approximate sampler – Algorithm 2 – which allows the HDP to be implemented with per-token sampling complexity of $\mathcal{O}[\min\{K_{d(i)}^{(m)}, K_{v(i)}^{(\Phi)}\}]$ which is the same as that of Pólya Urn LDA [25]. Compared to other approaches for the HDP, it offers the following improvements.

1. The algorithm is fully parallel in all of its steps.
2. The topic indicators z utilize all available sources of sparsity to accelerate sampling.
3. All steps not involving z are sampled with constant complexity with respect to data size.
4. The proposed approximate algorithm becomes exact as $N \rightarrow \infty$ and $K^* \rightarrow \infty$.

These improvements allow us to train the HDP via MCMC on larger corpora than any other published work we are aware of at the present. The data-parallel nature of our approach means that the amount of available parallelism increases with data size. This avoids the load-balancing-related scalability limitations of other methods that were recently pointed out by Gal and Ghahramani [10].

Nonparametric topic models are less straightforward to evaluate empirically than ordinary topic models. In particular, we found topic coherence scores [18] to be strongly affected by the number of active topics K , which causes preference for models with fewer topics and more semantic overlap per topic. We view development of summary statistics which are K -agnostic, as well as those measuring other aspects of topic quality such as overlap, to be a promising direction for future work. We are particularly interested in techniques that can be used to compare algorithms for sampling from the same model which are defined over fully disjoint state spaces, such as Algorithm 2 and the subcluster split-merge algorithm in Section 3.

Partially collapsed HDP can stabilize at a different local mode than fully collapsed HDP as proposed by Teh et al. [24]. There have been many attempts to improve mixing in that sampler [8, 14, 27], including the use of Metropolis-Hastings steps for jumping between modes [14] and related ideas. These techniques are largely complementary to our own, and can be explored in combination with the ideas presented here. HDP is a heavily multimodal target for which full posterior exploration is known to be difficult [8, 10], and sampling schemes are generally used more in the spirit of optimization than of traditional MCMC. We view MAP estimation-based analogues of ideas presented here as highly promising direction, since these may allow additional theoretical flexibility that may enable faster training.

Many of the ideas in this work are generic, and applicable to any topic model which is structurally similar to HDP’s GEM representation [24] given in Section 2. For example, one could consider using an informative prior for Ψ in lieu of $\text{GEM}(\gamma)$, potentially improving convergence and topic quality, or developing parallel schemes for other nonparametric topic models such as Pitman-Yor models [23] or tree-based models [5, 12, 20]. We leave such considerations to future work.

By leveraging parallelism and sparsity, our proposed techniques allow researchers to scale non-parametric topic models to larger datasets than previously considered feasible for MCMC or other methods possessing similar convergence guarantees. Our algorithm for the HDP is truly parallel and scales to a 768m-token corpus (PubMed) on a single multicore machine in under three days. We hope these contributions enable wider use of nonparametric Bayesian methods for large collections of text.

Acknowledgments

The research was funded by the Academy of Finland (grants 298742, 313122). The calculations presented above were performed using compute resources within the Aalto University School of Science and Department of Computing at Imperial College London. We also acknowledge the support of Ericsson AB.

References

- [1] A. Ahmed and E. P. Xing. Timeline: A Dynamic Hierarchical Dirichlet Process Model for Recovering Birth/Death and Evolution of Topics in Text Stream. In *Proceedings of the Twenty-Sixth Conference on Uncertainty in Artificial Intelligence*, 2010. Cited on page 1.
- [2] L. Ambrosio, N. Gigli, and G. Savaré. *Gradient flows: in metric spaces and in the space of probability measures*. Springer, 2008. Cited on page 12.
- [3] D. Blackwell and J. B. MacQueen. Ferguson distributions via Pólya urn schemes. *The Annals of Statistics*:353–355, 1973. Cited on page 2.
- [4] D. M. Blei, A. Y. Ng, and M. I. Jordan. Latent Dirichlet Allocation. *Journal of Machine Learning Research*, 3(1):993–1022, 2003. Cited on page 1.
- [5] D. M. Blei, T. L. Griffiths, and M. I. Jordan. The Nested Chinese Restaurant Process and Bayesian nonparametric inference of topic hierarchies. *Journal of the ACM*, 57(2):7, 2010. Cited on pages 1, 8.
- [6] V. I. Bogachev. *Measure Theory: Volume I*. Springer, 2007. Cited on page 12.
- [7] V. I. Bogachev. *Measure Theory: Volume II*. Springer, 2007. Cited on page 12.
- [8] J. Chang and J. W. Fisher III. Parallel sampling of HDPs using sub-cluster splits. In *Advances in Neural Information Processing Systems*, pages 235–243, 2014. Cited on pages 2, 6–8.
- [9] R. J. Connor and J. E. Mosimann. Concepts of independence for proportions with a generalization of the Dirichlet distribution. *Journal of the American Statistical Association*, 64(325):194–206, 1969. Cited on page 13.
- [10] Y. Gal and Z. Ghahramani. Pitfalls in the use of parallel inference for the Dirichlet process. In *International Conference on Machine Learning*, pages 208–216, 2014. Cited on pages 2, 8.
- [11] H. S. Heaps. *Information Retrieval: Computational and Theoretical Aspects*. Academic Press, 1978. Cited on page 6.
- [12] Y. Hu and J. Boyd-Graber. Efficient tree-based topic modeling. In *Proceedings of the 50th Annual Meeting of the Association for Computational Linguistics: Short Papers-Volume 2*, pages 275–279, 2012. Cited on pages 1, 8.
- [13] H. Ishwaran and L. F. James. Gibbs sampling methods for stick-breaking priors. *Journal of the American Statistical Association*, 96(453):161–173, 2001. Cited on pages 4, 5, 14, 15.
- [14] S. Jain and R. M. Neal. A split-merge Markov chain Monte Carlo procedure for the Dirichlet process mixture model. *Journal of Computational and Graphical Statistics*, 13(1):158–182, 2004. Cited on page 8.
- [15] A. Q. Li, A. Ahmed, S. Ravi, and A. J. Smola. Reducing the sampling complexity of topic models. In *Proceedings of the 20th International Conference on Knowledge Discovery and Data Mining*, pages 891–900, 2014. Cited on pages 2, 5.
- [16] M. Magnusson, L. Jonsson, M. Villani, and D. Broman. Sparse Partially Collapsed MCMC for Parallel Inference in Topic Models. *Journal of Computational and Graphical Statistics*, 27(2):449–463, 2018. Cited on pages 2, 3, 5, 6.
- [17] A. K. McCallum. MALLETT: A Machine Learning for Language Toolkit, 2002. URL: [HTTP://MALLETT.CS.UMASS.EDU](http://MALLETT.CS.UMASS.EDU). Cited on page 6.
- [18] D. Mimno, H. M. Wallach, E. Talley, M. Leenders, and A. McCallum. Optimizing semantic coherence in topic models. In *Proceedings of the Conference on Empirical Methods in Natural Language Processing*, pages 262–272, 2011. Cited on page 8.

- [19] D. Newman, A. Asuncion, P. Smyth, and M. Welling. Distributed algorithms for topic models. *Journal of Machine Learning Research*, 10:1801–1828, 2009. Cited on page 2.
- [20] J. Paisley, C. Wang, D. M. Blei, and M. I. Jordan. Nested hierarchical Dirichlet processes. *IEEE Transactions on Pattern Analysis and Machine Intelligence*, 37(2):256–270, 2015. Cited on pages 1, 8.
- [21] O. Papaspiliopoulos and G. O. Roberts. Retrospective Markov chain Monte Carlo methods for Dirichlet process hierarchical models. *Biometrika*, 95(1):169–186, 2008. Cited on page 4.
- [22] J. Pitman et al. *Combinatorial Stochastic Processes*. University of California, Berkeley, 2002. Cited on page 2.
- [23] Y. W. Teh. A hierarchical Bayesian language model based on Pitman-Yor processes. In *Proceedings of the 21st International Conference on Computational Linguistics and the 44th annual meeting of the Association for Computational Linguistics*, pages 985–992, 2006. Cited on pages 1, 8.
- [24] Y. W. Teh, M. I. Jordan, M. J. Beal, and D. M. Blei. Hierarchical Dirichlet processes. *Journal of the American Statistical Association*, 101(476):1566–1581, 2006. Cited on pages 1, 2, 6, 8.
- [25] A. Terenin, M. Magnusson, L. Jonsson, and D. Draper. Pólya Urn Latent Dirichlet Allocation: a doubly sparse massively parallel sampler. *IEEE Transactions on Pattern Analysis and Machine Intelligence*, 2018. Cited on pages 2–6, 8.
- [26] A. J. Walker. An Efficient Method for Generating Discrete Random Variables with General Distributions. *ACM Transactions on Mathematical Software*, 10(8):253–256, 1977. Cited on page 5.
- [27] C. Wang and D. M. Blei. A split-merge MCMC algorithm for the hierarchical Dirichlet process. *arXiv:1201.1657*, 2012. Cited on page 8.
- [28] C. Wang, J. Paisley, and D. Blei. Online variational inference for the hierarchical Dirichlet process. In *Proceedings of the Fourteenth International Conference on Artificial Intelligence and Statistics*, 2011. Cited on pages 2, 6.
- [29] S. Williamson, A. Dubey, and E. Xing. Parallel Markov Chain Monte Carlo for nonparametric mixture models. In *Proceedings of the 30th International Conference on Machine Learning*, pages 98–106, 2013. Cited on pages 2, 6.
- [30] L. Yao, D. Mimno, and A. McCallum. Efficient methods for topic model inference on streaming document collections. In *Proceedings of the 15th International Conference on Knowledge Discovery and Data Mining*, pages 937–946, 2009. Cited on page 2.
- [31] G. K. Zipf. *The Psycho-biology of Language: an Introduction to Dynamic Philology*. MIT Press, 2nd edition, 1968. Cited on page 1.

Appendix A: sufficiency of l and full conditional for b

Recall that the one-step-ahead conditional probability mass function in a Pólya sequence taking values in \mathbb{N} with concentration parameter α and base probability mass function Ψ is

$$p(z_i | z_{i-1}, \dots, z_1, \Psi) = \sum_{j=1}^{i-1} \frac{1}{i-1+\alpha} \mathbb{1}_{z_j}(z_i) + \frac{\alpha}{i-1+\alpha} \Psi_{z_i}. \quad (20)$$

Introducing the random variable

$$b_i \sim \text{Ber}\left(\frac{\alpha}{i-1+\alpha}\right) \quad (21)$$

we can express the one-step-ahead conditional distribution as

$$p(z_i | z_{i-1}, \dots, z_1, b_i, \Psi) = \mathbb{1}_{b_i=0} \sum_{j=1}^{i-1} \frac{1}{i-1} \mathbb{1}_{z_j}(z_i) + \mathbb{1}_{b_i=1} \Psi_{z_i}. \quad (22)$$

The joint probability mass function for $\mathbf{z} | \mathbf{b}, \Psi$ is then

$$p(\mathbf{z} | \mathbf{b}, \Psi) = \prod_{i=1}^N p(z_i | z_{i-1}, \dots, z_1, \mathbf{b}, \Psi) = \prod_{i=1}^N \left[\sum_{j=1}^{i-1} \mathbb{1}_{b_i=0} \mathbb{1}_{z_j}(z_i) + \mathbb{1}_{b_i=1} \Psi_{z_i} \right]. \quad (23)$$

Note that $\mathbb{1}_{b_i=0} = 1 \iff \mathbb{1}_{b_i=1} = 0$ and vice versa. Thus each term in the product for $\mathbf{z} \mid \mathbf{b}, \Psi$ only has one component, and we may express $\mathbf{z} \mid \mathbf{b}, \Psi$ as

$$p(\mathbf{z} \mid \mathbf{b}, \Psi) = \prod_{\substack{i=1 \\ b_i \neq 1}}^N \underbrace{\sum_{j=1}^{i-1} \frac{1}{i-1} \mathbb{1}_{z_j}(z_i)}_{\text{doesn't enter posterior}} \prod_{\substack{i=1 \\ b_i=1}}^N \prod_{k=1}^{\infty} \Psi_k^{\mathbb{1}_k(z_i)} \quad (24)$$

where we have re-expressed the probability mass function of Ψ in a form that emphasizes conjugacy. Thus for any prior, the posterior will only depend on the likelihood of the values of z_i for which $b_i = 1$. The sufficient statistic is

$$l_k = \sum_{\substack{i=1 \\ b_i=1}}^N \mathbb{1}_{z_i=k}. \quad (25)$$

Next, for a given $i' \in \{1, \dots, N\}$, we can calculate the posterior of a component $b_{i'}$ as

$$\mathbb{P}(b_{i'} = 1 \mid \mathbf{z}, \Psi, \mathbf{b}_{-i'}) \propto \left(\frac{\alpha}{i' - 1 + \alpha} \right) \prod_{\substack{i=1 \\ b_i \neq 1}}^N \sum_{j=1}^{i-1} \frac{1}{i-1} \mathbb{1}_{z_j}(z_i) \prod_{\substack{i=1 \\ b_i=1}}^N \Psi_{z_i} \quad (26)$$

$$\propto \alpha \Psi_{z_{i'}} \quad (27)$$

$$\mathbb{P}(b_{i'} = 0 \mid \mathbf{z}, \Psi, \mathbf{b}_{-i'}) \propto \left(\frac{i' - 1}{i' - 1 + \alpha} \right) \prod_{\substack{i=1 \\ b_i \neq 1}}^N \sum_{j=1}^{i-1} \frac{1}{i-1} \mathbb{1}_{z_j}(z_i) \prod_{\substack{i=1 \\ b_i=1}}^N \Psi_{z_i} \quad (28)$$

$$\propto \sum_{i=1}^{i'-1} \mathbb{1}_{z_i}(z_{i'}) \quad (29)$$

where we have divided both expressions by

$$\frac{1}{i' - 1 + \alpha} \prod_{\substack{i=1 \\ b_i \neq 1 \\ i \neq i'}}^N \sum_{j=1}^{i-1} \frac{1}{i-1} \mathbb{1}_{z_j}(z_i) \prod_{\substack{i=1 \\ b_i=1 \\ i \neq i'}}^N \Psi_{z_i} \quad (30)$$

which is constant with respect to $b_{i'}$. Note that full conditionally, we have $b_i \perp\!\!\!\perp b_{i'}$ for $i \neq i'$. This gives the desired expressions and concludes the derivation.

Appendix B: proof of Proposition 1

Here we calculate the posterior distribution under a GEM prior and discrete likelihood. Since we are working in a nonparametric setting, we begin by making precise what we actually mean when we speak of conditional probability.

Definition 2 (Regular conditional probability measure). *Let (Θ, \mathcal{C}) and (Y, \mathcal{Y}) be measurable spaces. A function $\pi_{\theta|y} : \mathcal{C} \times Y \rightarrow [0, 1]$, written $\pi_{\theta|y}(\cdot \mid \cdot)$, is called a regular conditional probability measure iff the following hold.*

1. For all $A_\theta \in \mathcal{C}$, the map $\pi_{\theta|y}(A_\theta \mid \cdot)$ is \mathcal{Y} -measurable.

2. For all $y \in Y$, the map $\pi_{\theta|y}(\cdot \mid y)$ is a probability measure.

Result 3. *Let (Θ, \mathcal{C}) and (Y, \mathcal{Y}) be measurable spaces. Let $\pi_\theta : \mathcal{C} \rightarrow [0, 1]$ be a probability measure and $\pi_{y|\theta} : \mathcal{Y} \times \Theta \rightarrow [0, 1]$ be a regular conditional probability measure. Then there exists a unique probability measure $\pi_{y,\theta} : \mathcal{C} \otimes \mathcal{Y} \rightarrow [0, 1]$ such that*

$$\pi_{y,\theta}(A_\theta \times A_y) = \int_{A_\theta} \pi_{y|\theta}(A_y \mid \theta) d\pi_\theta(\theta). \quad (31)$$

Moreover, for all measurable f we have that

$$\int_{\Theta \times Y} f(\theta, y) d\pi_{y,\theta}(\theta, y) = \int_{\Theta} \int_Y f(\theta, y) d\pi_{y|\theta}(y \mid \theta) d\pi_\theta(\theta). \quad (32)$$

Proof. Ambrosio et al. [2], Section 5.3. See also Bogachev [6], Theorem 3.3.1. ■

Result 4 (Disintegration Theorem). *Let (Θ, \mathcal{G}) and (Y, \mathcal{Y}) be complete separable metric spaces. Let $\pi_{y,\theta} : \mathcal{G} \otimes \mathcal{Y} \rightarrow [0, 1]$ be a probability measure, and let $\pi_y = \pi_{y,\theta}(\cdot \times Y)$. Then there exists a π_y -a.e. unique regular conditional probability measure $\pi_{\theta|y} : \mathcal{G} \times Y \rightarrow [0, 1]$ such that*

$$\pi_{y,\theta}(A_\theta \times A_y) = \int_{A_y} \pi_{\theta|y}(A_\theta | y) d\pi_y(y). \quad (33)$$

Moreover, for all measurable f we have that

$$\int_{\Theta \times Y} f(\theta, y) d\pi_{y,\theta}(\theta, y) = \int_Y \int_{\Theta} f(\theta, y) d\pi_{\theta|y}(\theta | y) d\pi_y(y). \quad (34)$$

Proof. Ambrosio et al. [2], Theorem 5.3.1. See also Bogachev [7], Corollary 10.4.15. ■

Together, these results say that given a prior and a likelihood, the joint distribution is uniquely determined. If our state space is sufficiently regular, this in turn gives existence of the posterior distribution, and almost everywhere uniqueness with respect to the marginal measure. For conjugate models, we may calculate the posterior via finite-dimensional distributions, because the conditionals of the marginals are equal to the marginals of the conditionals. Our posterior's finite-dimensional distributions are not analytic, so we instead work with an approximating sequence. Specifically, we show that if we introduce a sequence of approximating priors, and consider the induced sequence of approximating posteriors, then with sufficient continuity this sequence converges to the true posterior.

Proposition 5. *Let $\Theta = \prod_{k=1}^{\infty} \Theta_k$ be a complete separable metric space, let \mathcal{G} be its cylindrical σ -algebra, and let (Y, \mathcal{Y}) be a countable discrete space. Let π_θ be a probability measure, and let $\pi_{y|\theta}$ be a regular conditional probability measure. Let $\pi_{\theta|y}$ be their associated regular conditional probability measure given by disintegration. Suppose we have a sequence of measures $(\pi_\theta^{(K)})_{K \in \mathbb{N}}$ such that $\pi_\theta^{(K)} \rightarrow \pi_\theta$ weakly. For each $\pi_\theta^{(K)}$, let $\pi_{\theta|y}^{(K)}$ be the associated regular conditional probability measures given by disintegration. Assume for any bounded function $f(y)$ that the bounded function $\theta \mapsto \int_Y f(y) d\pi_{y|\theta}(y | \theta)$ is continuous. Then we have $\pi_{\theta|y}^{(K)} \rightarrow \pi_{\theta|y}$ weakly for all y .*

Proof. By definition of weak convergence, we have

$$\int_{\Theta} g(\theta) d\pi_\theta^{(K)}(\theta) \rightarrow \int_{\Theta} g(\theta) d\pi_\theta(\theta) \quad (35)$$

for all bounded continuous g . Let $f(y)$ be a bounded function, and let $f(\theta)$ be a bounded continuous function. Taking $g(\theta) = f(\theta) \int_Y f(y) d\pi_{y|\theta}(y | \theta)$, which is bounded continuous by assumption, and applying Result 3 yields

$$\int_{\Theta \times Y} f(\theta) f(y) d\pi_{\theta,y}^{(K)}(\theta, y) \rightarrow \int_{\Theta \times Y} f(\theta) f(y) d\pi_{\theta,y}(\theta, y) \quad (36)$$

and in particular, by letting $f(\theta) f(y) = f(y)$ and integrating out θ , we have $\pi_y^{(K)} \rightarrow \pi_y$ weakly. Every discrete metric space is complete, and since Y is countable it is separable. Applying the Disintegration Theorem – Result 4 – yields

$$\int_Y \int_{\Theta} f(\theta) f(y) d\pi_{\theta|y}^{(K)}(\theta | y) d\pi_y^{(K)}(y) \rightarrow \int_Y \int_{\Theta} f(\theta) f(y) d\pi_{\theta|y}(\theta | y) d\pi_y(y) \quad (37)$$

for any bounded function f . Since Y is a discrete space, we may rewrite the above integrals as summations with respect to the probability mass functions $p_y^{(K)}$ and p_y , which gives

$$\sum_Y f(y) p_y^{(K)}(y) \int_{\Theta} f(\theta) d\pi_{\theta|y}^{(K)}(\theta | y) \rightarrow \sum_Y f(y) p_y(y) \int_{\Theta} f(\theta) d\pi_{\theta|y}(\theta | y). \quad (38)$$

Taking $f(y)$ to be an indicator, and noting $\pi_y^{(K)} \rightarrow \pi_y$ implies $p_y^{(K)} \rightarrow p_y$ pointwise, we conclude

$$\int_{\Theta} f(\theta) d\pi_{\theta|y}^{(K)}(\theta | y) \rightarrow \int_{\Theta} f(\theta) d\pi_{\theta|y}(\theta | y). \quad (39)$$

Thus $\pi_{\theta|y}^{(K)} \rightarrow \pi_{\theta|y}$ weakly for all y and the claim follows. ■

Our strategy now is to find a sequence of finite-dimensional priors which converge to our infinite-dimensional prior, use them to calculate a sequence of finite-dimensional posterior distributions, and evaluate the limit of that sequence. We proceed to define such a sequence, beginning with some preliminary definitions for the given problem.

Definition 6 (Preliminaries). Let $(\Omega, \mathcal{F}, \mathbb{P})$ be a probability space. Let $S^\infty(\mathbb{N}) = \{\mathbf{x} \in [0, 1]^\infty : \sum_{i=1}^\infty x_i = 1\} \subset \ell^1$ be the probability simplex over \mathbb{N} . Let $N \in \mathbb{N}$. Let $\mathbf{x} \in \mathbb{N}^N$ be a vector. Let $\mathbf{l} \in N^\infty$ be its empirical distribution, i.e. $\mathbf{l} = \sum_{i=1}^N \mathbf{1}_{x_i}$ where $\mathbf{1}_{x_i}$ is equal to 1 for coordinate x_i and 0 for all other coordinate. Let $\gamma > 0$. Recall that \mathbb{N}^N and $S^\infty(\mathbb{N})$ are complete separable metric spaces when endowed with the discrete and ℓ^1 metrics, respectively. We associate each random variable $y : \Omega \rightarrow Y$ with its image probability measure $\pi_y(A_y) = [y_* \mathbb{P}](A_y) = \mathbb{P}[y^{-1}(A_y)]$, and each conditional random variable $\theta | y : \Omega \times Y \rightarrow \Theta$ with its image regular conditional probability measure $\pi_{y|\theta}(A_y | \theta) = [(y | \theta)_* \mathbb{P}](A_y) = \mathbb{P}[(y | \theta)^{-1}(A_y)]$, where the preimage is taken with respect to y .

Definition 7 (Discrete likelihood). For all $\Psi \in S^\infty(\mathbb{N})$, define the conditional random variable $\mathbf{x} | \Psi : \Omega \times S^\infty(\mathbb{N}) \rightarrow \mathbb{N}^N$ by its probability mass function

$$p(\mathbf{x} | \Psi) = \prod_{i=1}^N \prod_{k=1}^\infty \Psi_k^{\mathbf{1}_k(x_i)}. \quad (40)$$

We say $\mathbf{x} | \Psi \sim \text{Discrete}(\Psi)$.

Definition 8 (GEM). Let $\Psi : \Omega \rightarrow S^\infty(\mathbb{N})$ be a random variable defined by

$$\Psi_k = \varsigma_k \prod_{i=1}^\infty (1 - \varsigma_i) \quad \varsigma_k \sim \text{B}(1, \gamma). \quad (41)$$

We say $\Psi \sim \text{GEM}(\gamma)$.

We now introduce our finite-dimensional approximating prior and compute the posterior under it.

Definition 9 (Finite GEM). Let $\Psi : \Omega \rightarrow S^\infty(\mathbb{N})$ be a random variable defined by

$$\Psi_k = \varsigma_k \prod_{i=1}^{k-1} (1 - \varsigma_i) \quad \varsigma_k \sim \text{B}(1, \gamma) \quad \varsigma_K = 1. \quad (42)$$

We say $\Psi \sim \text{FGEM}(\gamma, K)$.

We now introduce our finite-dimensional approximating prior and compute the posterior under it.

Result 10. Let $\mathbf{z} | \Psi \sim \text{Discrete}(\Psi)$ and $\Psi \sim \text{FGEM}(\gamma, K)$. Then for any \mathbf{x} with associated counts \mathbf{l} , we have that $\Psi | \mathbf{x} : \Omega \times \mathbb{N}^N \rightarrow S^\infty(\mathbb{N})$ is a conditional random variable defined by

$$\Psi_k = \varsigma_k \prod_{i=1}^{k-1} (1 - \varsigma_i) \quad \varsigma_k \sim \text{B}(a_k^{(\Psi)}, b_k^{(\Psi)}) \quad \varsigma_K = 1 \quad (43)$$

where

$$a_k^{(\Psi)} = 1 + l_k \quad b_k^{(\Psi)} = \gamma + \sum_{i=k+1}^K l_i \quad (44)$$

and \mathbf{l} is the empirical distribution of \mathbf{x} . We say $\Psi | \mathbf{x} \sim \text{PGEM}(\gamma, \mathbf{l}, K)$.

Proof. It is shown by Connor and Mosimann [9] that $\Psi \sim \text{FGEM}(\gamma, K)$ is in fact a special case of the *generalized Dirichlet* distribution, which admits a general stick-breaking representation. Thus, its probability density function is

$$f(\Psi) \propto \Psi_K^{\gamma-1} \prod_{k=1}^{K-1} \left[\sum_{k'=1}^K \Psi_{k'} \right]^{-1} \quad (45)$$

which we have expressed in a simplified form. By conjugacy, for a given \mathbf{x} and associated l the posterior probability density is

$$f(\Psi | \mathbf{l}) \propto \Psi_K^{(\gamma+l_K)-1} \prod_{k=1}^{K-1} \left[\Psi_k^{(1+l_k)-1} \left[\sum_{k'=k}^K \Psi_{k'} \right]^{\gamma+\sum_{i=k}^K l_i - [(1+l_k)+\gamma+\sum_{i=k+1}^K l_i]} \right] \quad (46)$$

which is again a generalized Dirichlet admitting the necessary stick-breaking representation, which we have expressed in a form that emphasizes its posterior hyperparameters. ■

Remark 11. *It is now clear that the assumption $\mathbf{x} | \Psi \sim \text{Discrete}(\Psi)$ is indeed taken without loss of generality, because if we instead took $\mathbf{x} | \Psi$ to be given by a Pólya sequence, then by sufficiency the prior-to-posterior map induced by disintegration would be identical.*

Lemma 12. *Let $\Psi^{(K)} \sim \text{FGEM}(\gamma, K)$, let $\Psi \sim \text{GEM}(\gamma)$, and let $\pi_{\Psi^{(K)}}$ and π_{Ψ} be their respective image measures. Then we have $\pi_{\Psi^{(K)}} \rightarrow \pi_{\Psi}$ weakly.*

Proof. It is shown by Ishwaran and James [13] that $\Psi^{(K)} \rightarrow \Psi$ almost surely, which implies weak convergence of their image measures by the Portmanteau Theorem. ■

Lemma 13. *For any bounded continuous function $f : \mathbb{N}^N \rightarrow \mathbb{R}$, the bounded real-valued function $\Psi \mapsto \int_{\mathbb{N}^N} f(\mathbf{x}) d\pi_{\mathbf{x}|\Psi}(\mathbf{x} | \Psi)$ is continuous with respect to the ℓ^1 topology.*

Proof. We prove it is Lipschitz. Since $\mathbf{x} | \Psi$ is discrete, it admits a probability mass function, and we may write

$$\int_{\mathbb{N}^N} f(\mathbf{x}) d\pi_{\mathbf{x}|\Psi}(\mathbf{x} | \Psi) = \sum_{\mathbf{x} \in \mathbb{N}^N} f(\mathbf{x}) \prod_{i=1}^N \prod_{k=1}^{\infty} \Psi_k^{\mathbb{1}_k(x_i)} = \sum_{x_N=1}^{\infty} \dots \sum_{x_1=1}^{\infty} f(\mathbf{x}) \prod_{i=1}^N \Psi_{x_i}. \quad (47)$$

Note first that, by the triangle inequality,

$$\left| \prod_{i=1}^N \Psi_{x_i} - \prod_{i=1}^N \Psi'_{x_i} \right| = \left| \Psi_{x_1} \prod_{i=2}^N \Psi_{x_i} - \Psi'_{x_1} \prod_{i=2}^N \Psi'_{x_i} \right| \quad (48)$$

$$= \left| \Psi_{x_1} \prod_{i=2}^N \Psi_{x_i} - \Psi'_{x_1} \prod_{i=2}^N \Psi_{x_i} + \Psi'_{x_1} \prod_{i=2}^N \Psi_{x_i} - \Psi'_{x_1} \prod_{i=2}^N \Psi'_{x_i} \right| \quad (49)$$

$$= \left| (\Psi_{x_1} - \Psi'_{x_1}) \prod_{i=2}^N \Psi_{x_i} + \Psi'_{x_1} \left[\prod_{i=2}^N \Psi_{x_i} - \prod_{i=2}^N \Psi'_{x_i} \right] \right| \quad (50)$$

$$\leq |\Psi_{x_1} - \Psi'_{x_1}| \prod_{i=2}^N \Psi_{x_i} + \Psi'_{x_1} \left| \prod_{i=2}^N \Psi_{x_i} - \prod_{i=2}^N \Psi'_{x_i} \right| \quad (51)$$

$$\leq |\Psi_{x_1} - \Psi'_{x_1}| + \left| \prod_{i=2}^N \Psi_{x_i} - \prod_{i=2}^N \Psi'_{x_i} \right| \quad (52)$$

$$\leq \sum_{i=1}^N |\Psi_{x_i} - \Psi'_{x_i}| \quad (53)$$

where the second-to-last line follows because $0 \leq \Psi_i \leq 1$ for all i , and the last line follows by repeating the calculation inductively. Using this, we may write

$$\left| \int_{\mathbb{N}^N} f(\mathbf{x}) d\pi_{\mathbf{x}|\Psi}(\mathbf{x} | \Psi) - \int_{\mathbb{N}^N} f(\mathbf{x}) d\pi_{\mathbf{x}|\Psi'}(\mathbf{x} | \Psi') \right| = \quad (54)$$

$$= \left| \sum_{x_N=1}^{\infty} \dots \sum_{x_1=1}^{\infty} f(\mathbf{x}) \prod_{i=1}^N \Psi_{x_i} - \sum_{x_N=1}^{\infty} \dots \sum_{x_1=1}^{\infty} f(\mathbf{x}) \prod_{i=1}^N \Psi'_{x_i} \right| \quad (55)$$

$$\leq \|f\|_{\infty} \sum_{x_N=1}^{\infty} \dots \sum_{x_1=1}^{\infty} \left| \prod_{i=1}^N \Psi_{x_i} - \prod_{i=1}^N \Psi'_{x_i} \right| \quad (56)$$

$$\leq \|f\|_{\infty} \sum_{i=1}^N \sum_{x_i=1}^{\infty} |\Psi_{x_i} - \Psi'_{x_i}| \quad (57)$$

$$\leq \|f\|_{\infty} N \|\Psi - \Psi'\|_{\ell^1} \quad (58)$$

which establishes the claim. \blacksquare

The sequence of random variables $(\text{FGEM}(\gamma, K))_{K \in \mathbb{N}}$ defined above gives the sequence of probability measures needed to apply Proposition 5, and we are now ready to prove the main result.

Proposition 1. *Without loss of generality, suppose we have*

$$\Psi \sim \text{GEM}(\gamma) \quad \mathbf{x} | \Psi \sim \text{Discrete}(\Psi). \quad (59)$$

Then $\Psi | \mathbf{x}$ is given by

$$\Psi_k = \varsigma_k \prod_{i=1}^{k-1} (1 - \varsigma_i) \quad \varsigma_k \sim \text{B}(a_k^{(\Psi)}, b_k^{(\Psi)}) \quad a_k^{(\Psi)} = 1 + l_k \quad b_k^{(\Psi)} = \gamma + \sum_{i=k+1}^{\infty} l_i \quad (60)$$

where \mathbf{l} is the empirical distribution of \mathbf{x} .

Proof. In Lemma 12, we have given the convergent sequence $\Psi^{(K)} \sim \text{FGEM}(\gamma, K)$ needed to apply Proposition 5, and have verified the continuity condition in Lemma 13. From the proposition, conclude that the sequence of regular conditional probability measures associated with the conditional random variables $\Psi^{(K)} | \mathbf{x} \sim \text{PGEM}(\gamma, \mathbf{l}, K)$ given in Result 10 for any \mathbf{x} converges weakly $\pi_{\mathbf{x}}$ -a.e. to the desired posterior distribution $\Psi | \mathbf{x}$. The limit of this sequence is known: it is shown by Ishwaran and James [13] to converge almost surely to the conditional random variable given in equation (60). Since almost sure convergence of random variables implies weak convergence of their image measures, the claim follows. \blacksquare

Appendix C: quantile summary of topics for *CGCBIB*

Here we display a multi-quantile summary for *CGCBIB*. This is computed by ranking all topics with at least 100 tokens by their total number of tokens, computing the $\varpi = 100\%$, 75%, 50%, 25%, and 5% quantiles. We then compute the five topics closest to each quantile by number of tokens, and display their top-eight words.

CGCBIB partially collapsed $\varpi = 100\%$	110 702	58 811	27 084	21 215	19 832
	elegans	elegans	elegans	gene	mutations
	caenorhabditi	protein	genetic	elegans	gene
	nematode	caenorhabditi	molecular	sequence	mutants
	results	gene	development	protein	genes
	found	function	caenorhabditi	caenorhabditi	mutant
	show	proteins	nematode	amino	elegans
	observed	required	studies	cdna	caenorhabditi
specific	show	model	acid	alleles	
CGCBIB partially collapsed $\varpi = 75\%$	2 166	2 061	2 048	2 040	2 025
	germ	egl	emb	spe	wnt
	germline	egg	temperature	sperm	mom
	early	laying	mutants	fer	pop
	granules	serotonin	sensitive	spermatozoa	signaling
	cells	neurons	zyg	membrane	bar
	embryos	cat	maternal	spermatids	pathway
	somatic	dopamine	expression	spermatogenes	lin
line	mutants	embryonic	pseudopod	wrm	
CGCBIB partially collapsed $\varpi = 50\%$	930	916	915	900	893
	vit	binding	kinesin	growth	eat
	yolk	affinity	klp	survival	pharyngeal
	vitellogenin	site	transport	mortality	pharynx
	genes	activity	motor	population	pumping
	yp	sites	ift	rate	inx
	proteins	avermectin	cilia	populations	gap
	vpe	elegans	dynein	parameter	feeding
lrp	membrane	movement	size	junctions	
CGCBIB partially collapsed $\varpi = 25\%$	386	369	368	364	360
	mlc	dom	innate	vha	ife
	mel	effects	immune	atpase	cap
	myosin	humic	immunity	subunit	eife
	nmy	pyrene	abf	genes	capping
	chain	effect	lys	vacuolar	cel
	elongation	bioconcentrat	toll	subunits	gtp
	rho	dissolved	antimicrobial	atpases	isoforms
phosphatase	substances	pathway	type	rna	
CGCBIB partially collapsed $\varpi = 5\%$	141	141	140	140	136
	ubq	asp	da	ion	hcf
	gc	salmonella	cl	diet	cehcf
	tbp	poona	fli	relative	vp
	footprints	enterica	gs	xpa	ldb
	oscillin	clp	db	groups	cell
	tlf	serotype	glu	carbon	mammalian
	ubiquitin	necrotic	phospholipid	characteristi	phosphorylati
tata	mug	tg	atoms	neural	

CGCBIB	direct assignment $\varpi = 100\%$	65 059	41 005	33 714	27 221	22 813
		elegans	elegans	elegans	mutations	elegans
		caenorhabditi	genetic	caenorhabditi	elegans	gene
		protein	caenorhabditi	nematode	gene	sequence
		gene	nematode	results	mutants	caenorhabditi
CGCBIB	direct assignment $\varpi = 75\%$	2 442	2 409	2 394	2 332	2 284
		oxygen	germ	genes	elt	males
		oxidative	cells	gene	ges	male
		mev	line	expression	expression	sperm
		sod	germline	elegans	gut	hermaphrodite
CGCBIB	direct assignment $\varpi = 50\%$	1 213	1 211	1 207	1 203	1 143
		klp	ceh	proteins	smg	centrosome
		kinesin	pha	protein	mrna	zyg
		transport	pharyngeal	mass	mrnas	microtubule
		motor	gene	dimensional	splicing	centrosomes
CGCBIB	direct assignment $\varpi = 25\%$	664	658	642	638	630
		pkc	chemotaxis	mel	nsy	vha
		tpa	elegans	mlc	gcy	atpase
		kinase	nacl	myosin	asymmetry	jnk
		phorbol	defective	nmy	aser	isoforms
CGCBIB	direct assignment $\varpi = 5\%$	400	390	390	389	389
		irp	elements	bli	duplication	nex
		iron	ltr	ia	sas	hcf
		mammalian	retrotranspos	pc	gene	annexin
		dehydrogenase	rnase	kex	locus	cehcf
CGCBIB	direct assignment $\varpi = 5\%$	400	390	390	389	389
		zn	open	kpc	centrosome	mammalian
		dehydrogenase	reading	proprotein	duplications	ahr
		adh	frame	ida	zyg	mitochondrial
		cytosolic	element	egl	cis	mitop

Appendix D: quantile summary of topics for *NeurIPS*

Here we display a multi-quantile summary for *NeurIPS*. This is computed by ranking all topics with at least 100 tokens by their total number of tokens, computing the $\varpi = 100\%$, 75%, 50%, 25%, and 5% quantiles. We then compute the five topics closest to each quantile by number of tokens, and display their top-eight words.

NeurIPS partially collapsed $\varpi = 100\%$	182 743	162 355	129 745	52 356	44 155
	system	function	number	model	training
	information	case	result	neural	set
	approach	result	small	result	data
	set	term	values	system	test
	problem	parameter	order	activity	performance
	research	neural	large	input	number
	computer	form	effect	pattern	result
single	defined	high	function	error	
NeurIPS partially collapsed $\varpi = 75\%$	2 585	2 585	2 574	2 559	2 549
	genetic	delay	bengio	fig	matching
	algorithm	bifurcation	output	properties	model
	population	oscillation	dependencies	proc	point
	fitness	point	input	step	correspondenc
	string	stability	experiment	range	match
	generation	fixed	frasconi	structure	problem
	bit	limit	term	calculation	set
function	hopf	information	illinois	object	
NeurIPS partially collapsed $\varpi = 50\%$	1 310	1 309	1 309	1 297	1 295
	vor	routing	speaker	delay	memory
	storage	load	recognition	input	action
	anastasio	network	normalization	transition	states
	responses	path	male	window	agent
	velocity	packet	feature	width	sensing
	pan	traffic	female	connection	loop
	rotation	shortest	mntn	information	history
vestibular	policy	ntn	temporal	mdp	
NeurIPS partially collapsed $\varpi = 25\%$	748	748	746	739	735
	composite	psom	limited	tau	cmm
	mdp	robot	interconnect	hypothesis	speed
	action	camera	fan	mansour	particle
	elemental	set	shunting	growth	particles
	optimal	pointing	modularity	coefficient	pattern
	payoff	coordinates	collective	function	presence
	solution	basis	linear	stem	method
mdt	ritter	unit	large	card	
NeurIPS partially collapsed $\varpi = 5\%$	396	385	383	379	372
	morph	minimal	visualization	periodic	machine
	kernel	root	high	period	capacity
	parent	biases	low	coefficient	path
	human	attribute	diagram	primitive	trouble
	busey	remove	visualizing	homogeneous	high
	similar	rumelhart	graphic	tst	task
	exemplar	row	fund	mhaskar	increasing
distinctivene	exponential	window	chain	measures	

NeurIPS subcluster split-merge $\varpi = 100\%$	473 770	93 435	52 418	50 965	41 565
	network model learning function input neural algorithm set	network unit input learning training weight neural output	model neuron input network cell system unit visual	model data parameter network algorithm mixture function gaussian	function network bound dimension learning result number set
NeurIPS subcluster split-merge $\varpi = 75\%$	2 678	2 657	2 643	2 636	2 622
	learning critic function actor algorithm system control model	movement visual vector image model location eye map	motion unit direction model stage input network cell	learning algorithm action advantage system function policy control	cell correlation neuron model unit interaction firing set
NeurIPS subcluster split-merge $\varpi = 50\%$	1 032	1 028	1 013	1 009	1 006
	iiii cell network neural response model point fixed	cell spike unit function firing result transfer sorting	model response neural escape interneuron cockroach leg input	form word phone input network system training meaning	component algorithm sources analysis data noise orientation spatial
NeurIPS subcluster split-merge $\varpi = 25\%$	728	723	723	722	721
	aspect object view node learning network weight equation	element pairing grouping group saliency contour computation optimal	network neural constraint match learn problem initial row	input unit spike layer learning model predict prediction	traffic waiting elevator appeared application compared department found
NeurIPS subcluster split-merge $\varpi = 5\%$	509	507	506	503	503
	input output activation data encoded function hidden model	network neural task link food nodes output recurrent	network symbol vtp learning phrases sentences vpp classificatio	network equation neuron moment neural approximation ohira stochastic	network function adaptation algorithm prediction projection neural training

Appendix E: topics produced by Algorithm 2 on PubMed

Here we show top eight words for each topic together with total number of tokens assigned, which is shown at the top of each table. We display all topics containing at least eight unique word tokens.

PubMed	47 322 709	40 229 486	34 685 122	30 795 166	30 707 144
	care	age	model	cell	gene
	health	risk	data	expression	protein
	patient	children	system	growth	dna
	medical	year	time	protein	expression
	research	women	analysis	factor	sequence
	clinical	patient	effect	receptor	genes
	system	factor	test	kinase	rna
cost	population	field	beta	region	
PubMed	28 510 997	27 277 306	26 709 116	26 408 263	25 200 662
	cell	cancer	patient	rat	cell
	il	tumor	treatment	receptor	electron
	cd	patient	mg	effect	muscle
	mice	carcinoma	drug	neuron	tissue
	antigen	cell	effect	brain	fiber
	human	breast	therapy	activity	rat
	lymphocytes	survival	dose	stimulation	development
immune	tumour	day	induced	microscopy	
PubMed	24 856 624	24 750 437	24 607 618	24 482 090	22 956 810
	patient	patient	blood	patient	infection
	surgery	artery	pressure	disease	virus
	complication	heart	flow	clinical	hiv
	surgical	coronary	min	diagnosis	strain
	treatment	ventricular	effect	lesion	infected
	year	myocardial	exercise	brain	patient
	postoperative	cardiac	arterial	syndrome	positive
operation	left	heart	imaging	viral	
PubMed	22 095 623	21 838 239	21 363 408	20 887 061	20 828 980
	ca	structure	concentration	pregnancy	protein
	effect	binding	degrees	level	binding
	receptor	protein	samples	women	human
	channel	reaction	liquid	hormone	antibodies
	cell	acid	solution	day	acid
	calcium	interaction	assay	fetal	alpha
	concentration	compound	detection	infant	antibody
na	site	system	concentration	gel	
PubMed	20 106 260	19 788 488	18 675 096	17 163 327	16 440 018
	rat	bone	patient	gene	activity
	cell	patient	renal	mutation	acid
	effect	joint	liver	genetic	enzyme
	liver	muscle	transplantati	chromosome	liver
	mice	fractures	blood	analysis	concentration
	dose	hip	disease	genes	rat
	drug	year	acute	dna	enzymes
mg	implant	chronic	polymorphism	synthesis	

PubMed	16 136 164	14 201 063	13 706 016	13 191 158	13 105 245
	effect	diet	patient	strain	protein
	platelet	weight	disease	plant	membrane
	induced	intake	gastric	growth	cell
	oxide	food	asthma	acid	domain
PubMed	rat	body	test	bacteria	binding
	cell	effect	pylori	activity	receptor
	endothelial	acid	arthritis	cell	lipid
	activity	vitamin	chronic	species	membranes
PubMed	12 705 261	12 624 252	10 422 885	9 850 167	7 027 660
	insulin	species	exposure	skin	level
	glucose	population	concentration	patient	patient
	diabetes	infection	iron	eyes	ml
	cholesterol	animal	level	eye	control
PubMed	level	egg	water	retinal	serum
	diabetic	host	effect	laser	plasma
	plasma	parasite	exposed	visual	factor
	lipoprotein	malaria	lead	corneal	concentration
PubMed	6 130 945	644 182	2 264	1 325	104
	dental	sleep	ppr	pac	feather
	oral	caffeine	csc	foal	tieg
	teeth	tea	stretch	cpr	sorghum
	tooth	effect	pthrp	pacap	coii
PubMed	periodontal	theophylline	response	edm	phycocyanin
	treatment	night	br	speck	vanx
	salivary	coffee	gei	branchial	midrib
	gland	green	pth	lth	ifi
PubMed	104				
	steer				
	mca				
	persistence				
	buckwheat				
PubMed	dnak				
	eset				
	branding				
	akr				